JOURNAL OF CATALYSIS 146, 11–21 (1994)

Synthesis Gas Formation by Catalytic Oxidation of Methane in Fluidized Bed Reactors[1]

S. S. Bharadwaj and L. D. Schmidt[2]

Department of Chemical Engineering and Materials Science, University of Minnesota, Minneapolis, Minnesota 55455

Received July 6, 1993; revised September 14, 1993

The production of synthesis gas ($CO + H_2$) by the catalytic partial oxidation of CH_4 in air or O_2 in static fluidized beds at atmospheric pressure has been examined over Pt, Rh, and Ni catalysts coated on 100-μm α-Al_2O_3 beads. With CH_4/air feeds, CO and H_2 selectivities as high as 95% with >90% CH_4 conversion were obtained on Rh and Ni catalysts at contact times of 0.1–0.5 sec. Pt catalysts were found to have significantly lower selectivities and conversions, which may be due to more H_2O forming reactions or the slow steam reforming behavior of Pt. The optimal selectivities for all the three catalysts were improved by heating the reaction mixture above the autothermal reactor temperature and using O_2 instead of air. The selectivities and conversions were fairly constant over the range of contact times used. Probable reaction pathways for CH_4 oxidation in fluidized beds are discussed. © 1994 Academic Press, Inc.

1. INTRODUCTION

Much recent research (1) has been devoted to converting methane into liquid products. Methane can be converted to ethylene and ethane by oxidative coupling (2), and direct conversion to methanol has been reported (3). However all of these processes have relatively low conversions and selectivities. Another option is to convert methane to synthesis gas (a CO and H_2 mixture) and subsequently to methanol over Cu/ZnO or higher hydrocarbons through Fischer–Tropsch reactions on Fe, Co, Ru, and similar metals.

The dominant commercial method to produce synthesis gas is the steam reforming of natural gas and other light hydrocarbons which for methane produces a 3 : 1 H_2 : CO product mixture,

$$CH_4 + H_2O \rightarrow CO + 3H_2, \quad \Delta H = +49.2 \text{ kcal/mole.} \quad [1]$$

This reaction is carried out in a fuel fired tube furnace to provide the endothermic heat of this reaction. A typical steam reformer operates at 15 to 30 atm and 850 to 900°C with a Ni/Al_2O_3 catalyst and a superficial contact time (based on the feed gases at STP) of 0.5 to 1.5 sec (4), which corresponds to a residence time of several seconds. Depending on the end use, the H_2/CO ratio of the reformer product gases is often modified in shift reactors which utilize the water–gas shift reaction,

$$CO + H_2O \rightleftarrows CO_2 + H_2, \quad \Delta H = -9.8 \text{ kcal/mole.} \quad [2]$$

Both high-temperature water–gas shift reactors (~400°C using iron oxide/chromia catalysts) and low-temperature shift reactors (~200°C using a copper-based catalyst) have superficial contact times greater than 1 sec (5).

An alternate route for producing synthesis gas from methane which would directly give the desired 2 : 1 ratio is the direct oxidation of CH_4,

$$CH_4 + \tfrac{1}{2}O_2 \rightarrow CO + 2H_2, \quad \Delta H = -8.5 \text{ kcal/mole.} \quad [3]$$

While this reaction and these species are favored thermodynamically at $T > 900°C$, the selectivities are affected by the formation of H_2O in oxidation reactions which are much more exothermic,

$$CH_4 + \tfrac{3}{2}O_2 \rightarrow CO + 2H_2O, \quad \Delta H = -124.1 \text{ kcal/mole,} \quad [4]$$

and

$$CH_4 + 2O_2 \rightarrow CO_2 + 2H_2O, \quad \Delta H = -191.8 \text{ kcal/mole.} \quad [5]$$

Since the direct oxidation reaction is slightly exothermic, a reactor based on this reaction would be much more energy efficient than the energy intensive steam reforming process. Oxidation reactions are also much faster than reforming reactions, suggesting that a single-stage process for syngas generation would be a viable alternative to steam reforming, require much smaller reactors, and give higher throughput.

---

[1] This research was supported by the DOE under Grant DE-F02-88ER13878-AO2.

[2] To whom all correspondence should be addressed.

0021-9517/94 $6.00

All previous published studies of the partial oxidation of CH_4 (6–22) seem to have been done either in fixed beds or on monolith catalysts. Several studies (6, 12–16) have reported near equilibrium yields of CO and H_2 at temperatures between 700–1000°C and contact times of the order of 0.1 sec, and most of these authors (6, 12–16) postulate that the reaction pathway involves initial conversion of a fraction of the CH_4 feed to CO, CO_2 and H_2O, followed by steam reforming, CO_2 reforming, and reverse water–gas shift reactions. Recently, Choudhary *et al.* (18) reported non-equilibrium oxidative conversion of CH_4 to synthesis gas in a quartz microreactor over Ni/Al_2O_3 at low temperatures (<700°C) and contact times of ~7 msec. However, Dissanayake *et al.* (19) have recently suggested that the nonequilibrium selectivities observed by Choudhary *et al.* may have resulted due to small undetected hot spots which led to incorrect reactor temperature determination. We note that all of these processes use *tube wall furnaces* rather than *autothermal reactors*.

The production of CO and H_2 by the catalytic partial oxidation of CH_4 in air at atmospheric pressure was recently examined in this laboratory over Pt-coated and Rh-coated monolith catalysts in autothermal reactors at residence times between 10^{-4} and 10^{-2} sec (Hickman and Schmidt (20, 21); Hickman *et al.* (22)). CO selectivities above 95% and H_2 selectivities above 90% with >90% CH_4 conversion were reported for Rh catalysts.

The partial oxidation of methane in a fluidized bed for syngas generation has not to our knowledge been described in the literature, although Exxon has patented a process for steam reforming of methane with oxygen in a static fluidized bed reactor (23) and several related processes carry out similar reactions with steam and O_2 in fixed bed reactors (24). In this paper we present results on the partial oxidation of methane to produce synthesis gas in static fluidized beds over α-Al_2O_3 supported Pt, Rh, and Ni catalysts.

The CO selectivity, H_2 selectivity and CH_4 conversion are defined as

$$S_{CO} = \frac{F_{CO,out}}{F_{CO,out} + F_{CO_2,out}} \qquad [6]$$

$$S_{H_2} = \frac{F_{H_2out}}{F_{H_2,out} + F_{H_2O,out}} \qquad [7]$$

$$\text{Fractional CH}_4\text{ conversion} = \frac{F_{CH_4,in} - F_{CH_4,out}}{F_{CH_4,in}}, \qquad [8]$$

where F_j is the molar flow rate of species j.

The stoichiometric feed CH_4/O_2 ratio for total oxidation to CO_2 and H_2O is 0.5 (reaction [5]) and corresponds to 9.5% CH_4 in air or 33.3% CH_4 in O_2. For synthesis gas, the ideal feed CH_4/O_2 ratio is 2 (29.6% CH_4 in air or 66.7% CH_4 in O_2). At intermediate CH_4/O_2 feed ratios a mixture of CO, CO_2, H_2 and H_2O is obtained with complete conversion of the reactants. From stoichiometry, for a given feed composition, an increase in CO selectivity necessarily results in a corresponding decrease in the H_2 selectivity.

At equilibrium, a 2 : 1 CH_4/O_2 mixture is almost completely converted (>99.5% selectivity and conversion) to CO and H_2 at temperatures above 1000°C. However, at temperatures below 1000°C, coke formation should always take place. For leaner CH_4/O_2 mixtures, coke formation starts at lower temperatures.

2. EXPERIMENTS

2.1. *Apparatus*

The reactors were quartz tubes (1.9–3.2 cm diameter and 18–24 cm high) with expanded sections at the top (5–8 cm diameter and 8–10 cm high) for catalyst disengagement. A porous 40-μm quartz frit served as a gas distributor and support plate. The entire reactor was wound with high temperature heating tape and heavily insulated. All experiments for the results reported here were carried out in a 3.2-cm-diameter reactor. Gas flow into the reactor was controlled by mass flow controllers. The feed flow rates ranged from 0.5 to 2 slpm total flow, corresponding to 1.0 to 4 cm/sec superficial velocity (i.e., the velocity of the feed gases upstream from the catalyst) at room temperature and atmospheric pressure. The product gases were sampled just before the expansion with a gas tight syringe through a septum covered sample port. A coarse 175-μm pyrex frit was loosely fitted in the disengagement section to prevent blowout of fines.

The GC analysis was performed using two isothermal columns in series. For quantitative determination of the concentrations, standards were used for all species except H_2O, which was obtained most reliably from an oxygen atom balance. The mole number change due to reaction was determined by an atomic balance on nitrogen. The product gas carbon atom balances typically closed to within ±2% and the hydrogen atom balances to within ±5%.

Temperatures were monitored using two thermocouples, one before the quartz frit and one in the catalyst bed. Temperature measurements at different locations in the catalyst bed did not show a variation of more than 50°C. In order to determine the heat input through the heating tape, the feed gas temperature and the bed temperature were measured for a fixed power input without reaction by flowing air through the reactor.

2.2. *Catalyst Preparation*

All catalysts were prepared by deposition and decomposition of salts on low surface area, attrition resistant α-

Al_2O_3 supports. The alumina spheres, specially prepared for fluidization applications, had an average particle size ~80 μm with surface area of ~0.3 m^2/g. The packing density was ~1.1 g/cm^3 and the pore volume was ~0.2 cm^3/g (31). For metal deposition, the alumina was stirred in a salt solution of known concentration on a heating mantle until almost all the water evaporated. The wet mass was dried and then calcined for 2–3 hr at the appropriate temperature to decompose the salt. Catalysts with loadings of 0.25–2.0% by wt were prepared. Hexachloroplatinic acid and rhodium nitrate were used to deposit Pt and Rh, respectively. The Pt catalyst was calcined at 500–550°C and the Rh catalyst was calcined at a temperature of 300–350°C. Ni was deposited from nickel acetate, calcined at 470–480°C for 2–3 hr, and subsequently reduced in hydrogen at 500°C for 40 min. These loadings were calculated to correspond to continuous metal films ~8–14 Å thick on the surface of the alumina. The catalysts agglomerated above ~850°C for Ni and Pt, and above ~950°C for Rh, suggesting that external surfaces were in fact coated with metal. For results reported here, this did not occur because the temperatures were always lower than these temperatures.

2.3. *Catalyst Microstructure*

We used scanning electron microscopy (SEM) to examine the surface morphology of the catalysts. SEM micrographs of the alumina support both before and after impregnation showed that the beads were rough spheres ~100 μm in diameter with holes 3–5 μm in size distributed over the surface. The alumina crystal size was between 5 and 8 μm and clusters of small metal particles could be seen on the impregnated catalysts. There were no major detectable differences in the microstructure before and after use.

2.4. *Light-off*

Temperatures above 600°C are required for heterogeneous ignition of CH_4/air mixtures on Pt-foil or Pt on monolith catalysts (25, 20). In the fluidized bed it was difficult to light-off a stoichiometric mixture of CH_4 in air (9.5%) even at 700°C. In order to overcome this problem, stoichiometric mixtures of C_3H_8 in air (~4%) or NH_3 in air (~15%), which light-off at much lower temperatures (~370 and ~300°C, respectively) were used to ignite the catalyst. The bed was preheated in air or N_2 to ~350°C. The flow was then switched to a stoichiometric mixture of C_3H_8 in air or NH_3 in air. The catalyst would light off rapidly and the bed temperature would steadily increase to ~800°C in 3–4 min. CH_4 was then introduced and the C_3H_8 or NH_3 stream was simultaneously switched off. The catalyst bed would stay lit and attain a steady-state temperature after a few minutes, which was a function of the overall heat generation rate due to chemical reaction, the heat input through the heating tape, the heat energy (energy/time) carried in the product gases, and the rate of energy loss from the reactor by conduction, convection, and radiation. After steady state had been attained, the reactor temperature and conversions were typically constant for times up to several hours for fixed inlet conditions. Identical steady-state temperatures and product compositions could be repeated even after several changes in flow rates and feed conditions. Positioning of the thermocouple at different locations in the catalyst bed indicated that the bed was nearly isothermal and no hot spots were detected, which can be attributed to the good mixing action in the fluidized bed.

2.5. *Autothermal Behavior*

We observed that the catalyst would usually stay ignited after light-off even when there was no heat input, i.e., it would reach an autotherm. However, in small-scale equipment, heat losses are very high because of the high surface area to volume ratio. Moreover, in a fluidized bed the high heat transfer coefficients and backmixing promote heat losses. The autothermal temperatures were typically between 550–850°C for room temperature feed gases, depending on the stoichiometric composition of the CH_4/air mixture, the amount of catalyst in the reactor, and the reactor used. With richer CH_4 and air feeds, much less exothermic reactions take place which give lower autothermal temperatures. Low autothermal temperatures were also observed for smaller reactors as expected. In most experiments, the reactor was heated externally to raise the temperature of the reaction mixture to achieve better selectivities. The problem of heat losses is typical in small-scale equipment. A large-scale reactor, on the other hand, is expected to operate at higher autothermal temperatures, eliminating the need for additional heat input.

In our experiment, the fluidized bed runs autothermally because the catalyst exhibits ignition and extinction behavior characteristic of autothermal systems. The catalyst ignites at a particular temperature for the stoichiometric feed composition, attains a steady state higher temperature and extinguishes under certain conditions. Although additional heat input was needed at times, it was only necessary to counter the large heat losses. Extinctions were observed when the heat input was decreased for rich CH_4/air mixtures or when the feed composition was decreased below the stoichiometric feed composition for CH_4 (9.5%).

2.6. *Characteristics of the Fluidized Bed*

For our experiments, the fluidized bed was between the bubbling and turbulent regime over the range of flow rates used. In the bubbling regime there are two phases—the bubble phase and the emulsion phase. Bubbles 0.3–0.5 cm diameter were seen visually at lower flow rates. Calculations showed that the fluidization behavior of the catalyst was characteristic of aeratable powders (Group A) (30). No channeling was observed except when the catalysts agglomerated at high temperatures (>850°C for Ni and Pt and >950°C for Rh). Whenever this happened, the fluidization behavior was similar to that of cohesive powders (Group C).

At high flow rates closer to the turbulent regime there was more entrainment of fines. The turbulent regime is characterized by breakup of bubbles and more uniformity in the bed. There are several advantages to operation in the turbulent regime. The absence of complex bubble hydrodynamics makes scaleup relatively easier since the laboratory experiments more closely represent the behavior of a large scale reactor operated in the turbulent regime. Most of our experiments were close to this flow regime.

2.7. *Procedure*

All experiments for the results reported here were carried out in the same reactor (3.2 cm diameter and 30 cm total height) with the same amount of catalyst (~17.5 g). The Pt and Rh catalysts had loadings of 0.5% by wt while the Ni catalyst had a loading of 1% by wt. Thus, *identical conditions* (flow, heat input, and composition) *in the same reactor* allowed observations to be compared directly. The unfluidized bed depth was ~2 cm and the expansion was approximately a factor of two, which corresponded to a solid fraction of ~0.25. Depending on the total flow rate and bed expansion, the contact times at reaction temperatures (~850°C) were between 0.1 and 0.5 sec.

The product gas composition was measured as a function of CH_4 feed composition for a fixed flow rate and power input for all the three catalysts. The effect of temperature variation at the ideal feed gas composition for syngas (29.5%) was then measured by fixing the total flow and varying the power input. The effect of flow rate variation was measured by fixing the power input at 29.5% CH_4 in air.

3. RESULTS

3.1. *Variation with CH_4 Feed Composition*

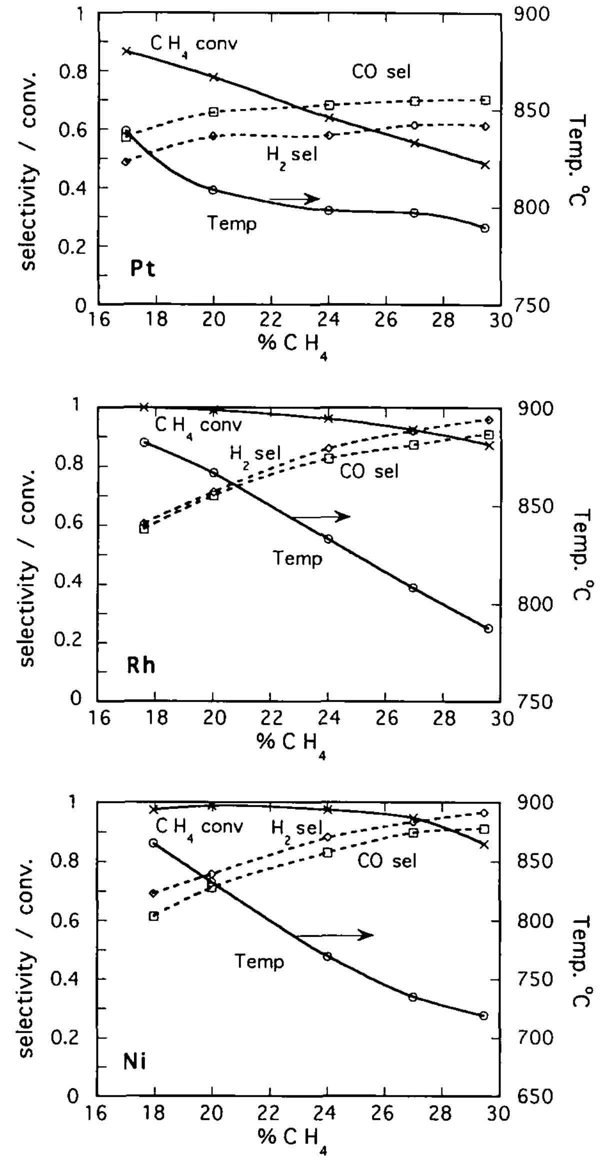

FIG. 1. CO selectivity, H_2 selectivity, CH_4 conversion, and temperature (°C) vs CH_4 feed composition in air at atmospheric pressure for Pt, Rh, and Ni catalysts (total flow rate = 1.2 slpm).

In Fig. 1 the CO and H_2 selectivities, CH_4 conversion, and bed temperatures for Pt, Rh, and Ni are shown as a function of CH_4 feed composition in air at a total flow rate of 1.2 slpm with a fixed power input. There are several common features in all the plots. The only detectable reaction products were CO, CO_2, H_2, and H_2O and the concentration of C_{2+} hydrocarbons was less than 0.05%. As the CH_4 feed composition is increased, the CH_4 conversion decreases and the CO and H_2 selectivities both increase. It can be seen that both selectivities are optimum near the ideal syngas feed composition of 29.5% CH_4. This increase in CO and H_2 selectivities is accompanied by a decrease in the bed temperature since the formation of these species is much less exothermic than the formation of H_2O and CO_2. The oxygen conversion remains essentially complete for all compositions on all catalysts.

From these data, it is apparent that Rh and Ni are much better catalysts for synthesis gas generation than Pt. Also, while on Pt the CO selectivity is always higher than the

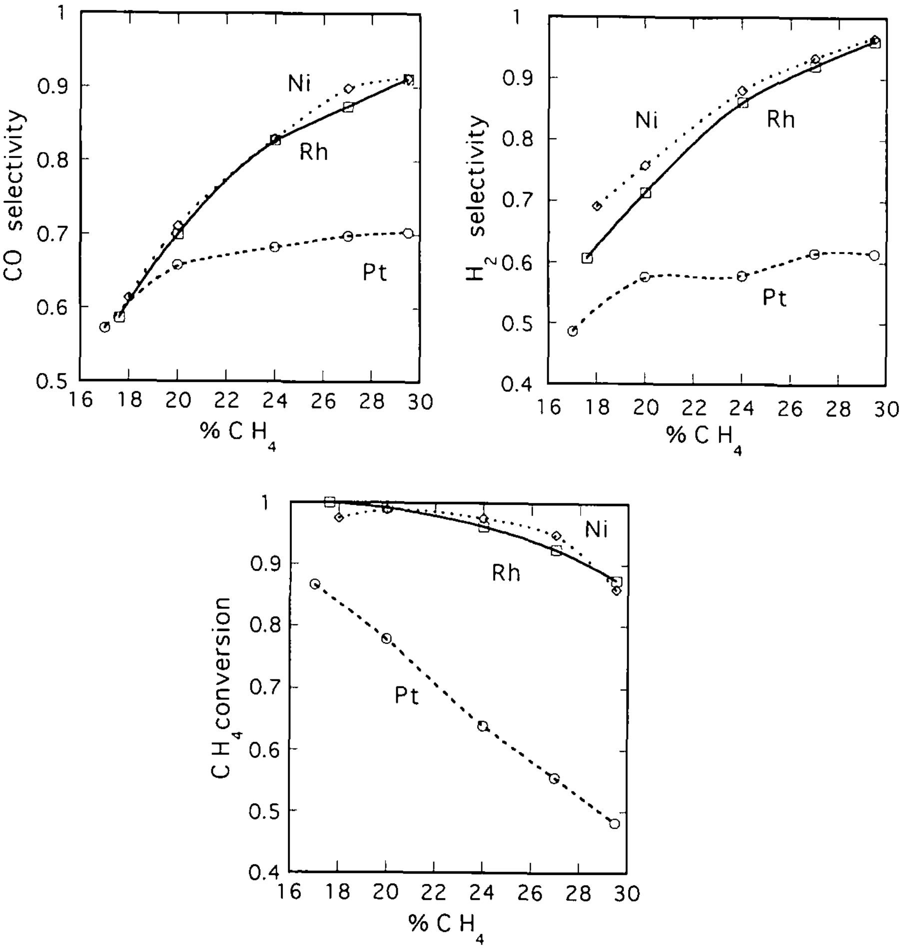

FIG. 2. Comparison of CO selectivity, H_2 selectivity, and CH_4 conversion as a function of CH_4 feed composition in air for Pt, Rh, and Ni catalysts (total flow rate = 1.2 slpm).

H_2 selectivity for the entire range of composition, on Rh and Ni it is reversed. The variation in bed temperature is also larger in the case of Rh and Ni compared to Pt which is expected because of the relatively flat selectivity curves for Pt. Calculations showed that the selectivities and conversions for Rh and Ni were within 10% of those predicted by thermodynamic equilibrium. A detailed comparison of the three catalysts is shown in Figs. 2–4.

3.2. Comparison of Pt, Rh, and Ni

Figure 2 compares the CO selectivity, H_2 selectivity, and CH_4 conversion for the three catalysts over the range of compositions studied.

At around 18% CH_4 feed composition, the CO selectivity is the same (~0.6) on all three catalysts. However, with richer methane feeds, while the CO selectivity increases to ~0.92 for Rh and Ni, it levels off at ~0.7 for Pt. Also, the CO selectivities are practically the same for Rh and Ni. On the other hand, there is a marked difference in the H_2 selectivities of the three at 18% feed composition. (~0.5 for Pt, ~0.6 for Rh, and ~0.7 for Ni). As the percentage of CH_4 is increased, the H_2 selectivity increases to ~0.96 for Rh and Ni but levels off at ~0.6 for Pt.

The CH_4 conversions for Rh and Ni are much higher than on Pt. On Rh and Ni it is essentially complete until about 20% CH_4 and then decreases to ~0.87. For Pt, the CH_4 conversion decreases from ~0.86 to ~0.48. The H_2/CO ratio is fairly constant with composition for the three metals. While Rh and Ni give the ideal H_2/CO ratio of ~2, it is lower on Pt, ~1.6.

3.3. Effect of Temperature

From the above data, it is clear that optimum H_2 and CO selectivities are obtained near the ideal syngas feed composition of 29.5% CH_4 in air. Experiments were thus performed at this feed composition at different temperatures (flow rate fixed at 1.2 slpm) by varying the heat

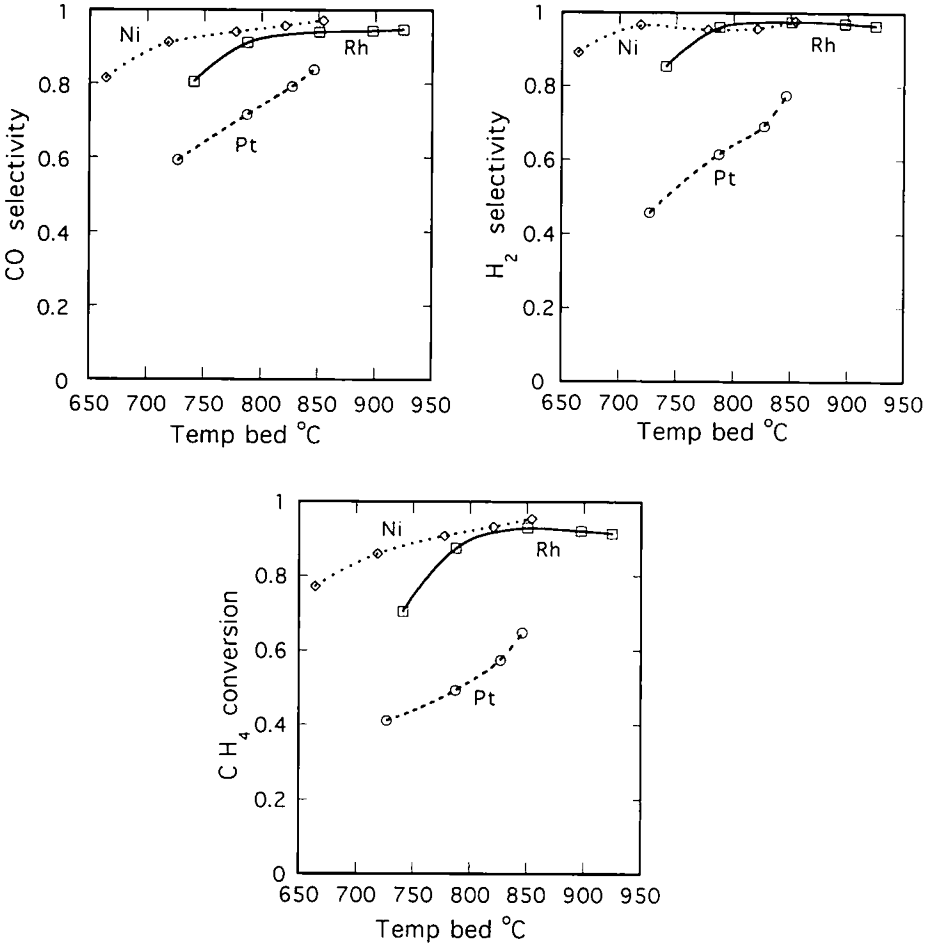

FIG. 3. Effect of bed temperature (°C) on CO selectivity, H_2 selectivity, and CH_4 conversion for Pt, Rh, and Ni catalysts (total flow rate = 1.2 slpm, 29.5% CH_4 in air).

input to see if the selectivities could be further improved. In Fig. 3, the CO selectivity, H_2 selectivity, and CH_4 conversion are plotted as a function of the measured bed temperature. The selectivities and conversions increase with temperature and level off beyond a certain temperature for Rh and Ni. For Pt the variation with temperature is large and no leveling off is observed.

Selectivities and conversions improve significantly with increased temperature. The highest CO selectivity obtained is ~0.95 on Rh and ~0.97 on Ni. Maximum H_2 selectivities of ~0.98 are obtained for both with CH_4 conversions of 0.93 and 0.95 for Rh and Ni, respectively. Pt is quite different giving a CO selectivity of ~0.84, a H_2 selectivity of ~0.78, and CH_4 conversion of ~0.65 at 850°C.

It seems that at higher temperatures the performance of Pt should improve although above ~850°C the Pt catalyst exhibited a change in fluidization characteristics in that particles agglomerated and produced channeling of the gases. The same phenomenon was observed on Rh and Ni but these effects are not crucial in these experiments because good performance was achieved at lower temperatures. A reduced metal loading would probably reduce this problem.

3.4. *Effect of Flow Variation*

Experiments were also performed to determine the effect of flow velocity on the performance, as shown in Fig. 4. The flow rates were varied from 0.7 to 2.0 slpm at the CH_4 feed composition of 29.5% and fixed power input. As before, Rh and Ni are better than Pt. All the curves are relatively flat but all begin to exhibit drops in H_2 and CO selectivities and lower CH_4 conversion at the lowest flow rates, just as was observed with monoliths (20). The selectivities are fairly constant over the range of flow rates used and we were unable to attain sufficiently high flow rates to observe the expected decrease in CH_4 conversion. Although the conversion for Ni (~0.91) and Pt (~0.56) does not change much, the conversion for Rh decreases from 0.94 to 0.8.

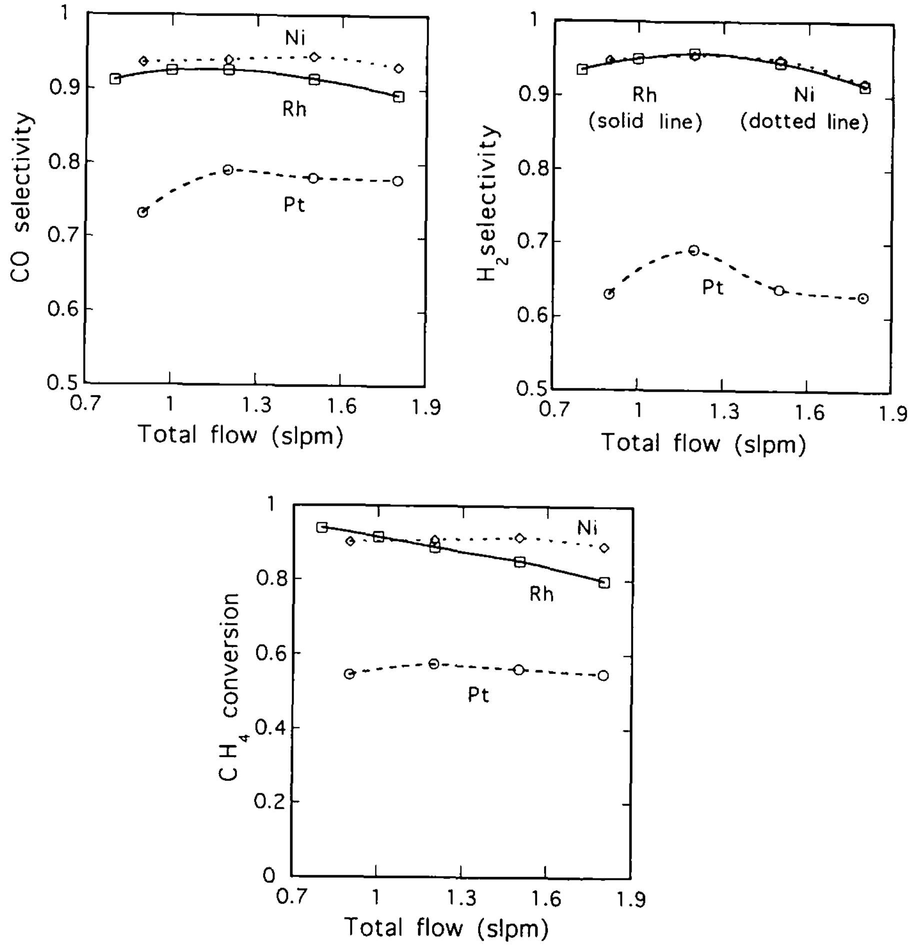

FIG. 4. Effect of flow rate (slpm) on CO selectivity, H_2 selectivity, CH_4 conversion for Pt, Rh, and Ni catalysts (29.5% CH_4 in air).

Higher flow velocities correspond to reduced contact times and smaller reactors for the same throughput. However, in static fluid beds there is a limit to the shortest contact time that can be achieved without significant catalyst entrainment and shorter times require a riser reactor with catalyst circulation. We expect that good performance could probably be achieved with much lower contact times in a properly designed riser reactor.

3.5. *Air versus O_2*

Experiments were also performed using pure O_2 instead of air. Data for experiments over the 0.5% Rh catalyst using both air and O_2 are shown in Fig. 5. For all these experiments a total flow rate of 1.2 slpm was maintained with a fixed power input. Since the same total flow rate was used as in the air experiments, the comparison between the air and O_2 experiments is at identical contact times. It can be seen that in the absence of the N_2 diluent, the selectivities, conversion and temperature are all higher. It was not possible to go below a CH_4/O_2 ratio of 1.4 with O_2 because flame flashback along with small explosions were observed upstream of the quartz frit.

3.6. *Effect of H_2O in Feed*

The effect of addition of steam in the feed was studied at a CH_4/O_2 ratio of 2 : 1 for a fixed total flow rate and power input. Figure 6a shows the observed CO selectivity and CH_4 conversion as a function of the H_2O (% vol) in the feed. Increasing the H_2O in the feed increases the CH_4 conversion which is >99% for greater than 20% H_2O. The CO selectivity which is ~0.96 in the absence of H_2O, decreases to 0.48 at 32% H_2O. The water–gas shift (WGS) reaction is,

$$CO + H_2O \rightleftarrows CO_2 + H_2, \quad \Delta H = -9.8 \text{ kcal/mole}. \qquad [9]$$

In Fig. 6b, the equilibrium constant K_{WGS} at the measured bed temperature and the experimental ratio $(P_{H_2}\,P_{CO_2})/(P_{H_2O}\,P_{CO})$ are plotted as a function of percentage of H_2O

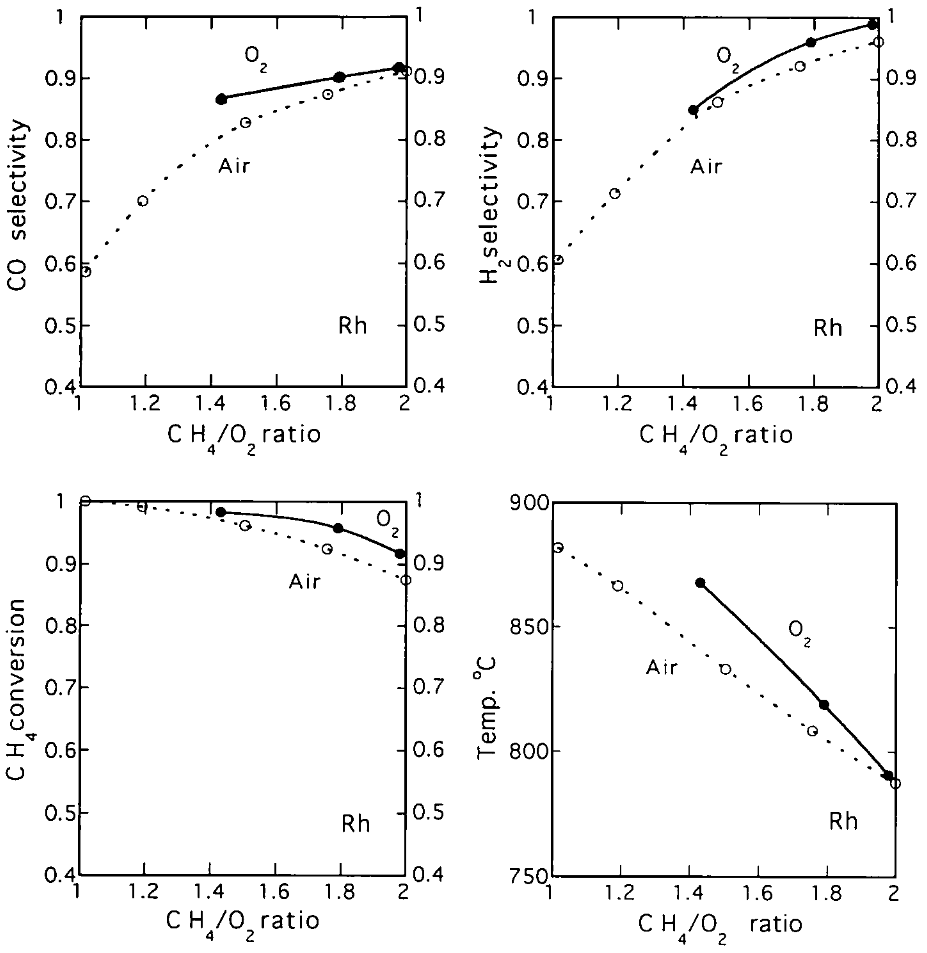

FIG. 5. Air vs O_2: comparison of CO selectivity, H_2 selectivity, CH_4 conversion, and temperature (°C) as a function of CH_4/O_2 ratio (catalyst ~0.5% Rh/Al_2O_3, total flow = 1.2 slpm).

in the feed to determine the approach to water gas shift equilibrium.

3.7. Stability

We ran experiments for ~20 hr on the Rh catalyst and for ~10 hr on the Pt and Ni catalysts and observed no deactivation except for Ni under certain conditions which are described later.

At a temperature of 700°C for a CH_4 feed composition of 29.5%, thermodynamics predicts ~3.5% solid graphite at equilibrium. This suggests that ~16.4% of the carbon in the CH_4 feed could end up as coke or soot and produce ~9 g of carbon (more than half the weight of the catalyst bed) over a period of 5 hr and at a flow rate of 1.2 slpm. At 800°C, thermodynamics predicts ~1.9 g of carbon over this period.

However, we did not see any evidence of carbon formation on the catalyst surfaces or soot deposition on the walls above the reactor. Moreover, there was no deterioration in the performance of the catalysts over the times used which should have occurred had there been continuous coke formation.

While no operational problems were observed with Pt and Rh catalysts, the Ni catalyst did exhibit some transients before the precautions required in its use were understood. It was found that the Ni catalyst would completely lose its activity if exposed to an oxidizing environment at temperatures above 600°C. The initially dark brown catalyst turned light green which was probably Ni-aluminate. Although rich CH_4/air mixtures were used during steady operation, oxide formation was likely while switching from C_3H_8 to CH_4 during light-off. It would almost inevitably take place when the CH_4 flow was stopped for shutdown, which would expose the catalyst to air at high temperatures until it cooled to room temperature. Shutdown could not be accomplished by removing air because, if the catalyst was allowed to cool down in CH_4, coke formation would take place. We then found that the catalyst could be completely recovered without any observable loss of activity by exposing it to H_2 or NH_3

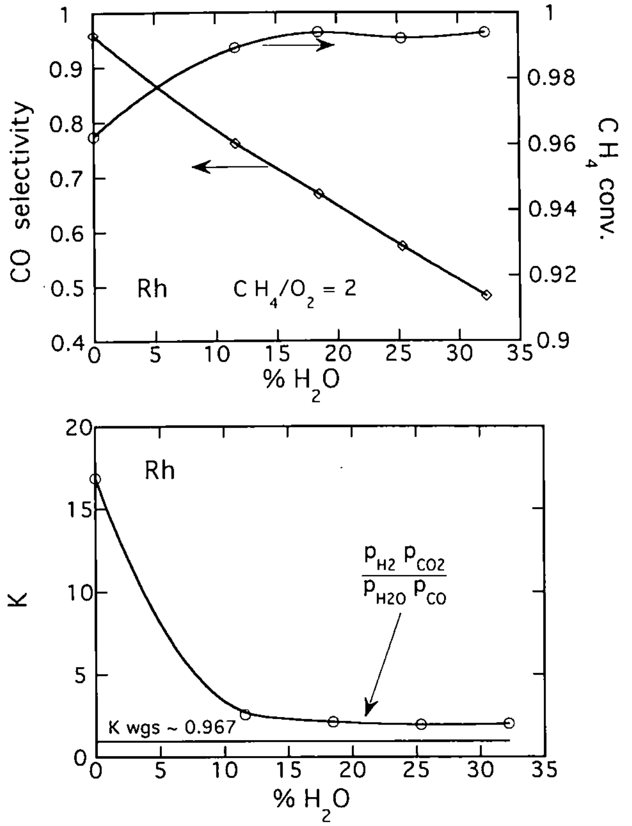

FIG. 6. (a) Effect of steam in feed on CO selectivity and CH_4 conversion (catalyst ~0.5% Rh/Al_2O_3, total flow = 1.2 slpm, 29.5% CH_4 in air). (b) Water-gas shift equilibrium constant and $(P_{H_2}\,P_{CO_2})/(P_{H_2O}\,P_{CO})$ vs % H_2O (by vol.) in feed (catalyst ~0.5% Rh/Al_2O_3, total flow = 1.2 slpm, 29.5% CH_4 in air).

for a short time (2–3 min) at high temperatures (>500°C). However, the reactor would take a very long time to cool down (~1 hr), and passing pure H_2 or NH_3 over the catalyst for such a long period was not a good option. In order to overcome this problem, the reactor was preheated in nitrogen before light-off, and during shutdown the CH_4 and air flows were stopped and the reactor allowed to cool down in nitrogen. Care was taken while switching valves so as to never leave the catalyst in an oxidizing environment. However, related experiments with Ni-coated monoliths (27) indicate significant metal loss at 900 to 1000°C, and eventual metal loss may be a problem with Ni catalysts in this reactor configuration.

3.8. Homogeneous versus Heterogeneous Reactions

We believe that results reported here correspond to heterogeneous partial oxidation of CH_4 in which all reactions take place on the catalyst surface. This is because, first, we did not see any flames in the catalyst bed. Second, when a 29.5% CH_4 in air mixture was passed over a heated bed of pure α-Al_2O_3 at 750°C, almost all the CH_4 passed through unreacted. Third, there were no C_2 hydrocarbons in the product gases, which for our atmospheric pressure experiments are good indicators of the possible presence of gas phase reactions.

In early experiments, we used an alumina cloth 4–5 cm thick instead of a fritted quartz disc as a support plate. We then could sometimes see reaction taking place on the alumina cloth as the CH_4/air mixture would ignite in the alumina section before reaching the fluidized bed. The entire alumina cloth would emit a bright yellow glow and the bed temperatures would drop, giving lower selectivities. This led us to change over to a quartz frit support 2 mm thick for the catalyst bed.

With air, the reactor could be operated safely even at the CO_2/H_2O stoichiometry (9.5%), and no flames and explosions were observed. We did however, see minor explosions and flames flash back upstream of the quartz frit when using O_2. This always occurred when the inlet temperature of the premixed CH_4/O_2 mixture exceeded ~650°C which would happen either at low flow rates or CH_4/O_2 ratios lower than 1.4. At low flow rates, the flame velocity exceeds the flow velocity and the premixed gases back-light. At low CH_4/O_2 ratios, the inlet temperature exceeds the ignition temperature of the premixed mixture causing it to ignite homogeneously. These reaction conditions were carefully avoided.

4. DISCUSSION

4.1. Comparison with Previous Experiments

Fixed beds. Most experiments examining partial oxidation of CH_4 with oxygen in fixed beds have been carried out in quartz microreactors ~1–4 mm in diameter with 20–50 mg of powder catalysts (12–19) with reactor tubes placed in a furnace or heater to thermostatically control temperatures.

Ashcroft and co-workers (12–15) studied methane oxidation to synthesis gas over a number of rare earth ruthenium oxides of the pyrochlore type ((Rare earth)$_2Ru_2O_7$) and several transition metals (Pt, Rh, Ru, Ni, Ir) supported on Al_2O_3. With a 2 : 1 : 4 $CH_4 : O_2 : N_2$ feed, $T >$ 750°C, and superficial contact times of 0.1 sec, CH_4 conversions in excess of 90% with selectivities in the range 94–99% were found for all catalysts, suggesting that all were nearly equal and that the active catalyst was supported metal. They suggested that the reaction pathway may involve initial conversion of some CH_4 to CO_2 and steam, followed by a sequence of steam reforming and reverse water–gas shift reactions to give equilibrium product yields.

Dissanayake *et al.* (16) examined the oxidation state and phase composition of a 25-wt% Ni/Al_2O_3 catalyst for CH_4 oxidation under O_2 deficient conditions as a function of axial position in the catalyst bed at atmospheric pressure and at temperatures between 450 and 900°C. Contact times of about 0.1 sec were required to give equilibrium yields of CO and H_2. CO selectivities approaching 95% and virtually complete conversion of CH_4 feed could be achieved at temperatures above 700°C. X-ray photoelectron spectroscopy and X-ray powder diffraction revealed that under operating conditions, the previously calcined catalyst bed consisted of three different regions. The first of these, contacting the initial $CH_4/O_2/He$ feed mixture was $NiAl_2O_4$ which had moderate activity for complete oxidation of CH_4 to CO_2 and H_2O. The second region was $NiO + Al_2O_3$, over which complete oxidation of CH_4 to CO_2 and H_2O occurred, resulting in an exotherm in this section. As a result of complete consumption of O_2 in the second region, the third portion of the catalyst bed consisted of a reduced Ni/Al_2O_3 phase. Formation of the CO and H_2 products corresponding to thermodynamic equilibrium at the catalyst bed temperature occurred in this final region via reforming reactions of the remaining CH_4 with the CO_2 and H_2O produced.

They also found that if the contact time was sufficiently decreased, breakthrough of unreacted O_2 occurred, causing all of the reduced nickel on the surface to reoxidize to the inactive $NiAl_2O_4$ phase. Reattainment of thermodynamic equilibrium could be achieved by regenerating the reduced Ni by raising the temperature above 750°C or by reducing the catalyst in H_2.

Choudhary *et al.* (18) recently reported successful operation at very high space velocities on a Ni/Al_2O_3 catalyst at low temperatures (<700°C). They found that at short contact times (~7 msec) the reaction is far from equilibrium and CO and H_2 selectivities higher than those predicted by equilibrium are obtained. No reaction pathway was suggested. However, Dissanayake *et al.* (19) have then pointed out that the apparent deviations of CH_4/O_2 reaction mixture products from thermodynamic equilibrium at high space velocities, as described by Choudhary *et al.* may have resulted due to a small undetected hot zone in their reactor and consequent incorrect determination of the true reaction temperature.

In our experiments in the fluidized bed we obtain near equilibrium selectivities and conversions for Ni and Rh catalysts at contact times between 0.1 and 0.3 sec. The major difference in our experiments is that the fluidized bed runs *autothermally* and attains its own temperature while a fixed temperature (ignoring reaction heating which could be significant) is imposed using a furnace in the above fixed bed experiments. The actual bed temperature and its axial variation is also not known accurately for the fixed bed experiments.

Monoliths. In the experiments of Hickman *et al.* (20–22), CH_4 oxidation was examined over Pt-coated and Rh-coated monoliths at very short contact times (10^{-4} to 10^{-2} sec). The monolith reactor was operated autothermally with feed temperatures between 25 and 460°C rather than at thermostatically controlled catalyst temperatures with conversions and selectivities very close to those obtained here in fluidized beds.

Hickman *et al.* suggested that the mechanism involved direct formation of H_2 initiated by CH_4 pyrolysis on the surface to give surface C and H species. The H adatoms dimerize and desorb as H_2 while the surface C atoms react with O adatoms and desorb as CO. However, any OH forming reactions on the surface would inevitably give H_2O. CO_2 would be formed by the reaction of adsorbed CO and O species. To explain the superiority of Rh over Pt for H_2 generation, they showed that since the activation energy for OH formation on Rh (20 kcal/mole) was higher than on Pt (2.5 kcal/mole), H adatoms were more likely to combine and desorb as H_2 on Rh than on Pt, on which the $O + H \rightarrow OH$ reaction was much faster.

They observed that almost all reaction took place in the first few mm of the monolith (contact times < 1 msec) with complete O_2 conversion to give H_2 and CO. In contrast to previous attribution of the syngas generation to a *sequence* of total oxidation followed by reforming, they demonstrated that H_2 and CO are *primary products* of the *direct* oxidation of methane at such short contact times.

Hickman and Schmidt (26) also modeled CH_4 oxidation using the CH_4 pyrolysis mechanism and an atmospheric pressure plug-flow reactor model with reaction parameters from literature. Their model agreed well with the experiments confirming that *direct oxidation* was the mechanism for oxidation on the monolith.

In ongoing experiments in this laboratory, Torniainen *et al.* (27) have studied methane oxidation on other metals supported on monoliths. Ni was found to give similar conversions and selectivities as Rh but exhibited deactivation. The performance of Pt was poor compared to Rh and Ni but better than that for Pd, Ru, Re, Fe, and Co.

These results for Pt, Rh, and Ni are similar to those shown here for the fluidized bed which was also run autothermally with preheated gases. However, the present experiments exhibit considerable *backmixing* in contrast to nearly plug flow in powder filled tubes or in monoliths.

4.2. *Reaction Pathways*

There are two possible reaction pathways for CH_4 oxidation in the fluidized bed, (1) direct oxidation to CO and H_2 or (2) total oxidation followed by reforming. Longer times compared to monoliths may allow more reforming while increased backmixing in the fluidized bed compared to plug-flow reactors may create more H_2O initially.

The first pathway is direct oxidation via methane pyrolysis as proposed by Hickman *et al.* (21, 22) for experiments with monolith catalysts at shorter contact times.

The low H_2 selectivities for Pt compared to Rh observed here conform very well with this mechanism.

The other reaction pathway may involve total oxidation of a part of the methane feed to CO_2 and H_2O followed by steam reforming, CO_2 reforming and water–gas shift reactions as proposed to explain microreactor syngas experiments (6, 12–16). Because of the significant backmixing of gases along with solids circulation, O_2 and H_2 will be present simultaneously, which should lead to more H_2O formation. Also, the contact times (0.2–0.3 sec) are sufficiently long for subsequent reforming and shift reactions to occur and give equilibrium CO and H_2 products. Rh and Ni also have a higher activity for steam reforming and methanation than Pt (28, 29), which would explain the lower CO and H_2 selectivities for Pt if reforming reactions play an important role.

We believe that homogeneous reactions involving free radicals do not play an important role in the reaction path because no flames were observed. Also C_2 hydrocarbons, the formation of which involves free radical chemistry along with surface reactions, were not detected in the product gases.

4.3. *Rh versus Ni*

Although Rh and Ni give similar selectivities and conversions, Ni is less stable toward oxidation and volatilization than Rh. Careful procedures must be followed during startup and shutdown to prevent exposure of the Ni catalyst to an oxidizing environment at high temperatures which deactivates the catalyst by forming $NiAl_2O_4$. Long-term stability of Ni may also be a problem because of volatilization. Therefore, Rh may be the catalyst of choice even though it is much more expensive than Ni.

5. SUMMARY

We have shown that hydrogen and carbon monoxide can be produced by CH_4 oxidation in a fluidized bed at contact times of 0.1–0.3 sec over Rh and Ni catalysts with selectivities higher than 95% and CH_4 conversion greater than 90%. We believe that reactions occur predominantly on the surface and that a direct catalytic oxidation process initiated by CH_4 pyrolysis appears to explain these results.

Since the fluidized bed was close to the turbulent mode, these results should simulate the behavior of a large scale reactor operating in the turbulent regime fairly closely, making scale-up relatively straightforward. Preliminary experiments show that good performance could probably be achieved with much lower contact times in a properly designed riser reactor with much higher throughputs.

These results have significant implications for CH_4 utilization. The high selectivities and conversions and the autothermal operation suggest that fluidized beds offer viable energy-efficient alternative reactor configurations for synthesis gas generation by the catalytic oxidation of methane.

REFERENCES

1. Shrivastava, R. D., Zhou, P., Steigel, G. J., Rao, V. U. S., and Cinquegrane, G., *Catalysis* **9,** 183 (1992).
2. Hutchings, G. J., Scurrell, M. S., and Woodhouse, J. R., *Chem. Soc. Rev.* **18,** 251 (1989).
3. Pitchai, R., and Klier, K., *Catal. Rev.-Sci. Eng.* **28,** 13 (1986).
4. Twigg, M. V. (Ed.), "Catalyst Handbook." Wolfe, London, 1989.
5. Satterfield, C. N., "Heterogeneous Catalysis in Industrial Practice." McGraw–Hill, New York, 1991.
6. Prettre, M., Eichner, C., and Perrin, M., *Trans. Faraday Soc.* **43,** 335 (1946).
7. Huszar, K., Racz, G., and Szekely, G., *Acta Chim. Acad. Sci. Hung.* **70,** 287 (1971).
8. Gavalas, G. R., Phichitcul, C., and Voecks, G. E., *J. Catal.* **88,** 54 (1984).
9. Korchnak, J. D., Dunster, M., and English, A., World Intellectual Property Organization, WO 90/06282 and WO 90/06297 (1990).
10. Hochmuth, J. K., *Appl. Catal. B: Environ.* **1,** 89 (1992).
11. Blanks, R. F., Wittrig, T. S., and Peterson, D. A., *Chem. Eng. Sci.* **45,** 2407 (1990).
12. Ashcroft, A. T., Cheetham, A. K., Foord, J. S., Green, M. L. H., Grey, C. P., Murrell, A. J., and Vernon, P. D. F., *Nature* **344,** 319 (1990).
13. Ashcroft, A. T., Cheetham, A. K., Green, M. L. H., and Vernon, P. D. F., *Nature* **352,** 225–226 (1991).
14. Vernon, P. D. F., Green, M. L. H., Cheetham, A. K., and Ashcroft, A. T., *Catal. Lett.* **6,** 181 (1990).
15. Jones, R. H., Ashcroft, A. T., Waller, D., Cheetham, A. K., and Thomas, J. M., *Catal. Lett.* **8,** 169 (1991).
16. Dissanayake, D., Rosynek, M. P., Kharas, K. C. C., and Lunsford, J. H., *J. Catal.* **132,** 117 (1991).
17. Bhattacharya, A. K., Breach, J. A., Chand, S., Ghorai, D. K., Hartridge, A., Keary, J., and Mallick, K. K., *Appl. Catal.* **80,** L1 (1992).
18. Choudhary, V. R., Rajput, A. M., and Prabhakar, B., *J. Catal.* **139,** 326 (1993).
19. Dissanayake, D., Rosynek, M. P., and Lunsford, J. H., *J. Phys. Chem.* **97,** 3644 (1993).
20. Hickman, D. A., and Schmidt, L. D., *J. Catal.* **138,** 267 (1992).
21. Hickman, D. A., and Schmidt, L. D., *Science* **259,** 343 (1993).
22. Hickman, D. A., Haupfear, E. A., and Schmidt, L. D., *Catal. Lett.* **17,** 223 (1993).
23. Eberly, Jr. P. E., Goetsch, D. A., Say, G. R., and Vargas, J. M., Exxon Research and Engineering Company, Eur. Pat. Appl. EP 335,668 (cl. COPB3/44), 04 Oct 1989, U.S. Appl. 174,174, 28 Mar 1988.
24. Haldor Topsoe A/S and Soc. Belge de l'Azote, *Hydrocarbon Process.* **67**(4), 77 (1988).
25. Balakrishna, A., Schmidt, L. D., and Aris, R., *Chem. Eng. Sci.* **49,** 11 (1994).
26. Hickman, D. A., and Schmidt, L. D., *AIChE J.*, **39,** 1164 (1993).
27. Torniainen, P., Chu, X., and Schmidt, L. D., in press.
28. Rostrup-Nielsen, J. R., *J. Catal.* **31,** 173 (1973).
29. Vannice, M. A., *J. Catal.* **37,** 449 and 462 (1975).
30. Geldart, D. (Ed.), "Gas Fluidization Technology." Wiley, New York, 1986.
31. Norton Chemical Process Products Corporation, Akron, Ohio.